Energy 135 (2017) 1–13

Contents lists available at ScienceDirect

Energy

journal homepage: www.elsevier.com/locate/energy

Directional liquefaction of biomass for phenolic compounds and *in situ* hydrodeoxygenation upgrading of phenolics using bifunctional catalysts

Junfeng Feng [a, b], Chung-yun Hse [b], Kui Wang [a], Zhongzhi Yang [a], Jianchun Jiang [a, *], Junming Xu [c, **]

[a] Institute of Chemical Industry of Forest Products, Chinese Academy of Forestry, National Engineering Lab. for Biomass Chemical Utilization, Key and Open Lab. on Forest Chemical Engineering, SFA, Key Lab. of Biomass Energy and Material, Nanjing 210042, China
[b] United States Department of Agriculture (USDA) Forest Service, Southern Research Station, Pineville, LA 71360, United States
[c] Research Institute of Forestry New Technology, Chinese Academy of Forestry, Beijing 100091, China

ARTICLE INFO

Article history:
Received 2 March 2017
Received in revised form
16 May 2017
Accepted 7 June 2017
Available online 9 June 2017

Keywords:
Directional liquefaction
In situ hydrodeoxygenation
Phenolic compounds
Bifunctional catalysts

ABSTRACT

Phenolic compounds derived from biomass are important feedstocks for the sustainable production of hydrocarbon biofuels. Hydrodeoxygenation is an effective process to remove oxygen-containing functionalities in phenolic compounds. This paper reported a simple method for producing hydrocarbons by liquefying biomass and upgrading liquefied products. Three phenolic compounds fractions (1#, 2#, and 3#) were separated from liquefied biomass with stepwise precipitation and extraction. Based on HSQC NMR analysis, three phenolic compounds fractions were mainly comprised of aromatic and phenolic derivatives. Three phenolic compounds fractions were hydrogenated and deoxygenated to cyclohexanes using bifunctional catalysts via *in situ* hydrodeoxygenation. During the *in situ* hydrodeoxygenation, we introduced bifunctional catalysts combined of Raney Ni with HZSM-5. The bifunctional catalysts showed high selectivity for removing oxygen-containing groups in biomass-derived phenolic compounds. And the hydrogen was supplied by aqueous phase reforming of methanol without external H_2. Additionally, the mechanism based on our investigation of *in situ* hydrodeoxygenation of phenolic compounds was proposed. During the *in situ* hydrodeoxygenation, the metal-catalyzed hydrogenation and acid-catalyzed hydrolysis/dehydration were supposed to couple together. Current results demonstrated that *in situ* hydrodeoxygenation using bifunctional catalysts is a promising and efficient route for converting biomass-derived phenolic compounds into fuel additives and liquid hydrocarbon biofuels.

1. Introduction

Due to the gradual depletion of conventional non-renewable resources and generation of greenhouse emissions, renewable energy sources are attracting extensive attention [1]. Lignocellulosic biomass is one of the most promising renewable energy sources for sustainable production of fuels and chemicals [2,3]. Waste lignocellulosic biomass, such as furniture manufacturing waste, paper production waste, and agricultural residues are carbon neutral and not fully utilized [4–6]. There are currently two main routes for transforming these waste biomass into renewable feedstocks and chemicals: biological conversion and thermochemical conversion [6,7]. Alternative thermochemical methods can convert solid biomass into liquid bio-crude, which includes liquefaction (heating with a solvent to obtain liquefied products) and fast pyrolysis (rapidly heating without air to obtain pyrolysis oil) [7–9]. As an important thermochemical conversion technology, liquefaction can provide an efficient pathway to convert solid biomass into liquefied oil [10]. Ideally, the liquefaction of biomass using organic solvents to obtain high added-value chemicals and fuels is a particularly important part of thermochemical conversion [11]. The liquefied bio-crude contains more than 200 compounds with different molecular weights and sizes [12,13]. The complex compounds in raw liquefied oil are chemically and thermally unstable with high oxygen and moisture content [14]. Thus, making liquefied oil

* Corresponding author.
** Corresponding author.
E-mail addresses: bio-energy@163.com (J. Jiang), lang811023@163.com (J. Xu).

http://dx.doi.org/10.1016/j.energy.2017.06.032
0360-5442/

economically sustainable is very important for the commercialization of biobased production [15].

Liquefied bio-crude is a complex mixture, contains renewable and valuable phenolic compounds such as 4-methoxyphenol, dimethylphenol, syringol, and catechol [16,17], and contains 30 wt% of lignin-derived phenolics, which are of high energy density [18]. Although many methods have been proposed for extracting phenolic compounds from bio-oil [19–23], their studies regarding characterization and fractionation of bio-oil were not focused on extraction of phenolics. Their work provided much helpful information on the composition of liquefied oil and the effect of extraction solvent selected on yield of phenols [19,20]. Molecular distillation is technically suitable for extraction and purification of thermally unstable substances [21,22] such as liquefied oil, but the method is not cost-effective because of the high vacuum and expensive equipment needed. Steam distillation by adding water vapour provides temperature lower than the common boiling points of phenolic compounds [23], but further purification is essential because the selectivity of phenolic compounds in the distillate is low (21.3%). Supercritical carbon dioxide extraction of liquefied oil is a good choice for pre-separation of phenolic compounds, because of the non-flammable and non-toxic characteristics of carbon dioxide and its low critical temperature (31.26 °C at 72.9 atm), however, the low phenols concentration (31%–41%) is an obvious drawback [24]. Another published method for separating phenolic compounds from bio-crude is organic solvent fractionation combined with an acidification-basification process [25], which unavoidably results in amount of salts. Although pyrolysis oil can be phase-separated into water-soluble and water-insoluble fractions by extraction with water, the upgraded and utilization of water-insoluble fractions is not clearly understood.

Hydrodeoxygenation is an effective technology for upgrading phenolic compounds into high energy hydrocarbons such as alkanes and hydrocarbons. Hydrodeoxygenation of lignin-derived model phenolic compounds to cyclohexanes and their derivatives with external H_2 has been reported in recent literatures [26–29]. For example, zeolite supported metal catalysts, such as Pt/HBeta [30], Ru/HBeta [18], Cu/HBeta [31], Ru/HZSM-5 [32], and Ni/HZSM-5 [33] have been widely used in the hydrodeoxygenation process with external H_2, for converting model phenolic compounds into cyclohexanes and hydrocarbons. Other dual-functional catalysts, such as Pd/C with liquid acid (H_3PO_4) [34] or solid acid (HZSM-5) [35] are also important catalyst components in present of external H_2 and water solvent for converting lignin-derived model phenolic compounds into hydrocarbons. These studies were focused on monomers and dimers model phenolic compounds with external H_2, which may not be applied to the real lignin-derived phenolic compounds from the complex components in bio-oil or liquefied bio-crude. The hydrodeoxygenation of model phenolic compounds with external H_2 has been mostly conducted at high H_2 pressure in a batch-wise autoclave (4–20 MPa) or in a continuous-flow fixed-bed reactor (5–10 MPa) [26]. The high H_2 pressure was required to give a high deoxygenation degree, but it saturated the aromatic ring before eliminating the oxygen groups [29]. These studies of model phenolic compounds are important for establishing the optimal conditions for converting phenolic-rich bio-crude into high quality biofuels. In an industrial bio-oil system, the highly active oxo-functionalized molecules also readily polymerize, which requires suitable catalytic technology and process to directly hydrodeoxygenate the bio-crude under mild conditions. Liquid hydrodeoxygenation donors such as alcohols and water are used during the hydrogenation process instead of external H_2. Vasiliadou [36] and Yfanti [37] investigated a tandem catalytic cycle of aqueous phase reforming of methanol for glycerol hydrodeoxygenation targeted to 1,2-propanediol formation. The hydrogen donor needed for glycerol hydrodeoxygenation was provided by *in situ* aqueous phase reforming of methanol. Ferrini [38] investigated the approach to catalytic biorefining of biomass to non-pyrolytic lignin bio-oil in 2-propanol and water over Raney Ni. The hydrogen generated from the aqueous phase reforming of 2-propanol, can effective transfer to the phenols. However, specific studies on the effects of the coupling aqueous-phase reforming of alcohols to the *in situ* hydrodeoxygenation of phenolic compounds and the application for *in situ* hydrodeoxygenation are still lacking.

Considering all of the above limitations, we have developed a simple method for separating the renewable phenolic compounds derived from liquefied biomass and upgrading these phenolic compounds into cyclohexane hydrocarbons suitable as fuel additives and bio-fuel. The separation method involved the development of stepwise precipitation and water-organic solvent extraction technology. In this work, we investigated the feasibility of using a water-organic solvent to extract renewable phenolic compounds from liquefied products. Therefore, we expect that this approach could be applicable for all thermochemical conversion methods of bio-crudes. The upgraded method of phenolic compounds was investigated on *in situ* hydrodeoxygenation with the aqueous phase reforming of methanol with bifunctional catalysts. The bifunctional catalysts combined Raney Ni with HZSM-5 can achieve the aqueous-phase reforming of methanol coupled with the *in situ* hydrodeoxygenation of phenolic compounds. The cyclohexane hydrocarbons were also obtained through a cascade bifunctional catalysed cleavage of C–O bonds in phenolic dimers. Overall, this study aimed to investigate the stepwise separation method and *in situ* hydrodeoxygenation process that can be efficient and economical design for converting waste lignocellulosic biomass into fuel additives and liquid hydrocarbon biofuels.

2. Experimental

2.1. Chemicals

All chemicals in the study were of analytical grade, commercially available, and used without further purification. The bamboo, bagasse, eucalyptus, pine, poplar, and straw used in the experiments were collected from a local farm (Jiangsu, China). The composition analysis results are shown in Table S1. All materials were dried under vacuum at 105 °C for 24 h and passed through a 40–50 mesh (size 300–425 μm) sieve. The materials were kept in sealed bag until needed, at which time small samples were dried further in an oven at 105 °C for 12 h.

2.2. Preparation three phenolic compounds fractions

Three phenolic compound fractions and glycoside compound fraction were obtained by a stepwise method and water-organic solvent extraction technology of liquefied products obtained from different biomass materials. The liquefied products were collected from a directional liquefaction, which were carried out in a high-pressure autoclave fitted with a thermocouple, stirring device, and a pressure gauge (0–30 MPa). 60 g biomass material was introduced into a solution of 420 g methanol with 1.5 g of sulfuric acid. The mixtures were heated in an autoclave at a specified temperature and stirred for a designated time period. When the reaction was complete, the autoclave was cooled to room temperature in a water bath. The liquefied liquid mixtures were removed from the autoclave and filtered through a membrane filter with a pore size of 0.8 μm. The filtrate was neutralized to pH = 7 using NaOH solution. The liquefied products were distilled under vacuum at 50 °C to remove and recycle the methanol, which left liquefied products (bio-oil) that did not contain methanol. The filter cake

(residue) was repeatedly washed with methanol to extract the residue as completely as possible. The residue was dried at 105 °C for 24 h.

The three phenolic compounds fractions and glycoside compounds fraction were obtained by water-organic solvent with a stepwise precipitation and extraction process. Deionized water was added into the liquefaction neutralized filtrate (liquefied products) with a weight ratio of 3:10. Insoluble pyrolytic lignin with high-weight molecular (phenolic compounds fraction 1#) in filtrate mixtures was precipitated by a centrifuge process. Then, the methanol was partly removed by distillation of the mixture liquid under vacuum at 50 °C, after which the lower-weight molecular fraction of pyrolytic lignin (phenolic compounds fraction 2#) was separated. Furthermore, 20 g ethyl acetate (EtOAc) was added into the mixture liquid (mixture liquid to EtOAc with a weight ratio of 1:1). While the methanol was completely removed, the liquefied mixtures were separated into water soluble phase and EtOAc soluble phase. The EtOAc soluble phase was distilled under vacuum at 45 °C to remove the EtOAc and to separate the lowest-weight molecular fraction of pyrolytic lignin (phenolic compounds fraction 3#). These three phenolic compound fractions of pyrolytic lignin were phenols separated from liquefied products (Fig. 1). The three parts of phenolic compounds were diluted with acetone for GC-MS analysis.

Besides, Eq. (1) was used to calculate the biomass conversion (on a weight basis).

$$\text{Conv. } (\%) = 1 - \frac{\text{weight of solid residue}}{\text{weight of materials}} \times 100\% \quad (1)$$

We discussed the results of scaled-up extraction including the mass balance of the whole directional liquefaction and extraction, extraction efficiency. The mass balance of liquefaction process included the weight of major products (three phenolic compounds fractions and glycoside compounds fraction) and the recovery of solvent. Furthermore, we investigated the GC-MS components of three phenolic compounds fractions and glycoside compounds fraction, 2D HSQC NMR analysis of three phenolic compounds fractions, GPC and FT-IR analysis of three phenolic compounds fractions and liquefied products, SEM, TG-DTG, and XRD analysis of biomass material and liquefied residue.

2.3. Preparation of catalysts

250 g NaOH solution (50 g NaOH solid fully dissolved in 200 mL deionized water) was added into a 500 mL three-necked round-bottom flask. Then 30 g Ni–Al alloy (Shandong Jiahong Chemical Co., Ltd.) was slowly added to the NaOH solution in round-bottom flask at the temperature of 50 °C. The solution was precipitated after 2 h of ultrasonic dispersion and magnetic stirring at 60 °C. The prepared solid was washed several times by deionized water until the pH = 7–8, and then washed on the filter by ethanol for removing water. The prepared Raney Ni catalyst was kept in ethanol until needed.

The HZSM-5 catalyst was prepared by repeated with ion-exchange of commercially available ZSM-5 zeolite (Catalyst Company of Nankai University) with a 10 wt% NH_4Cl solution at 80 °C with magnetic stirring. Each procedure lasted for 1 h, the used solution was substituted with fresh solution (1 g zeolite in 10 mL solution). The process was repeated 5–6 times, after which the solid was washed with deionized water on the filter for 4–5 times for removing Cl^-, and then dried at 120 °C for 12 h. The acid HZSM-5 catalyst was generated by activation at 450 °C in air for 8 h.

2.4. In situ catalytic hydrodeoxygenation of three phenolic compounds fractions

The *in situ* hydrodeoxygenation of three phenolic compounds fractions (2.0 g) were performed in a 100 mL stainless autoclave in the presence of 1.0 g Raney Ni and 1.0 g HZSM-5 bifunctional catalysts. In a typical experiment of the aqueous phase reforming of methanol, water (40 g) and methanol (10 g) were loaded into the autoclave. Then the autoclave was sealed and purged with N_2 for 3 times to exclude air, and the initial pressure (p_0) was raised to 0.1 MPa. An automatic controller was used to control the revolution of the stirrer (600 r/min) and the temperature of reactor. The reaction temperature was set at 220 °C with a heating rate of 5 °C/min, and the reaction time was 9 h after reaching the set temperature. After the reaction, the autoclave was cooled down to the room temperature, liquid and gas products were analyzed by GC-MS and GC, respectively.

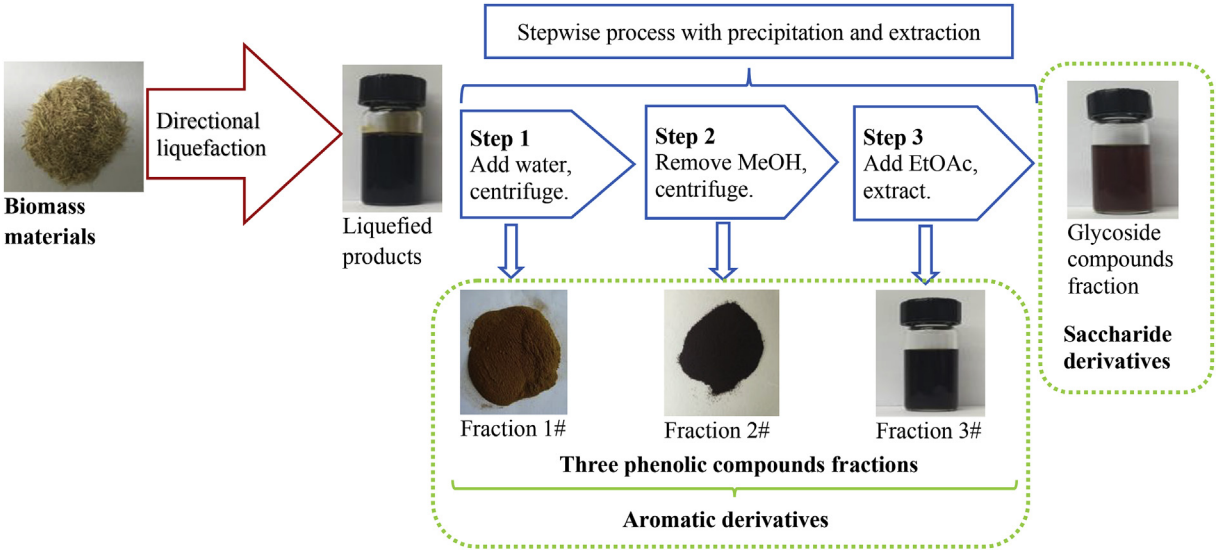

Fig. 1. Schematic of the procedures for phenolic compounds fractions from liquefied products.

2.5. Analysis methods

The main components analysis of liquefied products and phenolic compounds were conducted on a mass spectrometer (MS, Agilent 5975C VL MSD). The products were separated into their components using a gas chromatograph (GC, Agilent 7890A) equipped with a fused capillary column (HP-5, L = 30 m, inner diameter = 0.25 mm, and film thickness = 0.25 μm) with 5% phenyl methyl silox and 95% dimethylpolysiloxane as the stationary phase. Temperature programming was held at 25 °C for 5 min, heated to 240 °C at the rate of 10 °C/min, followed by 15 min at 240 °C. Injector temperature was maintained at 240 °C. The carrier gas was helium at a flow rate of 1.8 mL/min (linear velocity 45 cm/s) and 90 KPa inlet pressure was the carrier gas employed. The sample (0.2 μL) was injected neat with 1:20 split ratio at a split flow rate of 1.5 mL/min. The identification of the components of liquefied products and phenolic compounds were confirmed using total ion chromatograms as well as a fragmentation pattern. The MS detector was operated in the electron ionization mode (70 eV) with an ionization temperature of 220 °C. The mass spectra were recorded in electron ionization mode for *m/z* 50–550.

The molecular weights of three phenolic compounds fractions and liquefied products were measured by Gel Permeation Chromatography (GPC) using Waters-1515 system (USA) equipped with the manually packed column. GPC analysts were performed using the 20 μL injection volumes. Analysis was completed in 25 min. Tetrahydrofuran and polystyrene were used as solvent and internal standard, respectively.

Functional groups of liquefied products and phenolic compounds were measured using Fourier Transform Infrared Spectroscopy (FT-IR). The test ranged from 4000 to 300 cm^{-1}, with resolution greater than 0.4 cm^{-1}, ASTM standard linearity better than 0.1% T, and wave number accuracy greater than 0.01 cm^{-1}.

The structures of three phenolic compounds fractions were determined by Nuclear Magnetic Resonance (NMR) spectroscopy. ^{13}C–^{1}H correlation 2D Heteronuclear Single Quantum Coherence (HSQC) NMR was recorded on a Bruker DRX 500 NMR spectrometer that operated at 500 MHz. The spectral widths for the ^{1}H and ^{13}C dimensions were 8.5 and 120.0 ppm. The measurement was conducted in dimethyl sulfoxide (DMSO-d_6) solvent at 30 °C, and tetramethylsilane was used as the internal reference.

A NeoScope JCM-5000 scanning electron microscope (SEM) (5–10 kV accelerated voltage) was used to analyze the morphology of the raw material and liquefied residue in order to compare the effect of heating liquefaction treatments.

A thermogravimetric (TG, PerkinElmer) analyzer was used to analyze the raw materials and liquefied residue under N_2 atmosphere. The nitrogen flow rate was kept at about 250 mL/min at standard state. A sample weight of around 10 mg was used in every occasion and placed in a crucible. Initially, the material and residue were heated to 120 °C and kept for at least 30 min under the N_2 atmosphere to remove all the moisture from the material and residues. Afterwards, biomass material and liquefied residues sample were heated from 30 °C to 800 °C at a heating rate of 10 °C/min.

X-ray diffraction (XRD) patterns of the raw materials and liquefied residue were performed using an X′ RA instrument with monochromatic Cu/*Ka* radiation (λ = 0.154180 nm). The diffracted intensity was measured in a 2θ range from 10° to 60°, using a counting speed of 2°/min, with a step of 0.02°.

Eq. (2) was used to calculate the relative crystallinity of material and liquefied residue.

$$\text{Segal equation: } Cr(\%) = (I_{002} - I_{am})/I_{002} \times 100\% \quad (2)$$

Cr——Percentage degree of relative crystallinity.
I_{002}——(002) Crystal surface diffraction intensity, the maximum diffraction intensity.
I_{am}——The amorphous region diffraction scattering intensity of 2θ angle near 18°.

3. Results and discussion

3.1. Directional liquefaction of biomass and extraction of liquefied products

Ethyl acetate (EtOAc) is one of the most commonly-used solvents for extraction processes, and has been used to demonstrate many potential applications. In this work, we used H_2O and EtOAc solvents with stepwise precipitation and extraction to separate three phenolics and glycosides fractions from liquefied biomass products. The EtOAc can be removed and collected by distillation at low temperature and recycled for subsequent extraction.

We proposed the following basic scheme for using a water-organic solvent, new stepwise precipitation and extraction method to separate three phenolics fractions and glycosides fraction from liquefied products. The stepwise precipitation and extraction process is illustrated in Fig. 1. First, deionized water and high-speed centrifugation were used to separate water-insoluble phase compounds (fraction 1#). Second, switch the water and methanol to its hydrophilic form liquefied products to separate methanol-insoluble phase (fraction 2#) with the lowest-weight molecular phenols kept in the water phase. Third, use an organic solvent such as EtOAc to extract these phenolic compounds (fraction 3#) from the water phase. At the same time, the glycoside compound fraction in the water-soluble phase can be acquired in the extraction process with high purity.

3.1.1. Mass balance of whole directional liquefaction and extraction

The mass balance of whole liquefaction and extraction was shown in Table 1. The main components of gas products in biomass liquefaction were shown in Table S2. The conversion of lignocellulosic biomass material was according to the mass of liquefied products (without methanol). The conversion of biomass material was mostly more than 80%. About 20 g methanol was lost in the conversion of 60 g biomass with 420 g methanol. A part of reduced methanol went into the bio-oil, and some was lost as dimethyl ether or other gaseous products such as H_2, CO, and CO_2.

After the stepwise precipitation and extraction process, the weights of three phenolic compounds fractions that separated from six material liquefied oil were remarkably different. The recovered liquefied products of bamboo in the three phenolic compounds fractions and glycoside compounds fraction, calculated without methanol was 48.05 g in total, which was 94.16% of the starting liquefied products (51.03 g). The rest was lost in the deionized water and part of it was kept in the recycled ethyl acetate and methanol. Fraction 1# and fraction 2# were the major fractions of the solid phenolic compounds. In bamboo liquefaction and extraction process, they accounted for 14.23% and 19.02% of the liquefied products (without methanol) mass, respectively. Fraction 3# was extracted by EtOAc solvent accounting for 7.87% of liquefied products (without methanol) mass. Compared with other biomass materials, bamboo, bagasse, and pine were better liquefied and extracted.

3.1.2. Main components of three phenolic compounds from biomass liquefied products

The main components of three phenolic compounds fractions from bamboo, bagasse, eucalyptus, pine, poplar, and straw liquefied products are shown in Table 2 and Table S3. Many kinds of phenolic

Table 1
Mass balance of different biomass material liquefaction and solvent extraction.

Biomass	Biomass conversion (%)	Liquefied products (g)					Solid residue (g)	Extraction efficiency[a] (%)
		Mass in phenols fraction			Glycosides	Recovery of methanol		
		1#	2#	3#				
Bamboo	85.05	6.84	9.14	3.78	28.29	398.51	8.97	94.16
Bagasse	85.30	6.02	9.45	3.92	29.18	387.06	8.82	94.90
Eucalyptus	82.70	5.08	8.93	3.54	29.04	401.33	10.38	93.89
Pine	84.02	5.25	9.02	3.90	28.14	385.42	9.59	91.86
Poplar	80.33	5.04	8.46	3.77	28.09	400.18	11.80	94.11
Straw	79.15	4.68	8.88	3.51	27.48	385.42	12.51	93.60

Reaction conditions: sulfuric acid 1.5 g, material 60 g, methanol 420 g, temperature 200 °C, time 10 min.
[a] Extraction efficiency = mass of phenolic compounds and glycosides/mass of liquefied products (without methanol).

compounds were detected in the products, such as 2-methoxy-4-propyl-phenol, 4-methoxy-guaiacol, 4-propyl-2,6-dimethoxy-phenol, 4-hydroxy-3-methoxyphenyl-2-ethanol, 4-(3′-methoxy-4′-hydroxy)-phenyl-2-carboxylate, 4-methoxy-2-hydroxy-benzoate, and methyl 3-(4-hydroxy-3-methoxyphenyl)-acrylate. This result indicated that the bamboo was effectively degraded into low-weight molecular chemicals during the liquefaction process. The directional liquefaction of biomass was not only simply the degradation of hemicellulose and cellulose with recalcitrant crystalline structure, but also included the depolymerisation of high polymerization lignin. The decomposition of the lignin structure in the biomass material had a similar mechanism by cleaving the dominant linkages including 4-O-5, β-O-4, and dibenzodioxin unit [39]. The methanol solvent with −OH functions as a nucleophile attacked the electrophilic C adjacent to the glycosidic bond in cellulose and hemicellulose. As a result, the electrons moved towards the oxonium ion, created a neutral hydroxyl group and a good leaving group by cleaving the C–O bond.

Three phenolic compound fractions included phenolic monomers, dimers with various functionalities, especially methyl, methoxy, aldehydes, ketones, esters, and other complex propyl groups. Three phenolic compounds fractions from different biomass materials were remarkably different (Table S3). The components and distributions of three phenolic compounds fractions from the same liquefied products were also significantly different. Fraction 1# were mainly consisted of 4-methoxy-guaiacol, 4-hydroxy-3-methoxyphenyl-2-ethanol, 1-(4-hydroxy-3-methoxyphenyl) ethanone, 4-(3′-methoxy-4′-hydroxy)-phenyl-2-carboxylate, (E)-methyl 3-(4-hydroxy-3-methoxyphenyl) acrylate, and a part of phenolic dimers. The mainly components of fraction 2# compounds were eugenol, 4-propyl-2,6-dimethoxy-phenol, 4-hydroxy-3-methoxy-phenyl-2-ethanol, 1-(4-hydroxy-3-methoxy-phenyl) ethanone, 4-(3′-methoxy-4′-hydroxy)-phenyl-2-carboxylate, 4-methoxy-2-hydroxy benzoate, and little phenolic

Table 2
Main components of three phenolic compounds fractions from bamboo liquefied products.

R.T (min)	Identification by GC-MS	Area (%)[a]		
		1#	2#	3#
	Phenolic compounds	**79.96**	**82.74**	**85.51**
10.67	2-Methyl-phenol	3.29	–	6.19
13.08	Guaiacol	1.77	2.33	4.67
13.47	4-Methyl-guaiacol	–	3.17	8.29
16.69	3-Methyl-guaiacol	2.30	3.89	6.23
17.31	2-Methoxy-4-propylphenol	4.21	6.39	4.22
18.09	4-Methoxy-guaiacol	3.89	7.22	14.74
19.46	Eugenol	3.19	14.23	9.72
20.27	4-Propyl-2,6-dimethoxyphenol	5.89	8.34	6.17
20.95	4-Hydroxy-3-methoxyphenyl-2-ethanol	10.46	12.02	8.33
23.66	1-(4-hydroxy-3-methoxyphenyl)ethanone	12.93	7.68	–
25.39	Vanillin	4.78	–	9.88
26.47	4-(3′-methoxy-4′-hydroxy)-phenyl-2-carboxylate	5.33	7.93	6.22
27.23	Methyl-4-hydroxy-3-methoxybenzoate	2.13	–	8.21
29.80	Methyl-2-(4-hydroxy-3-methoxyphenyl)acetate	3.49	2.30	–
30.62	(3,4-dimethoxyphenyl)-methoxy-methanol	2.87	0.94	–
31.52	4-Methoxy-2-hydroxybenzoate	3.77	6.03	4.58
31.98	(E)-Methyl 3-(4-hydroxy-3-methoxyphenyl) acrylate	6.22	4.32	7.21
33.5–35.0	Phenolic dimers	8.50	3.45	–
	Others	7.16	6.44	5.81
6.39	Furfural	–	–	1.16
8.53	5-Hydroxymethylfurfural	–	–	2.60
10.94	β-Methoxy-2-furanmethanol	0.57	2.17	1.02
17.64	2-Naphthalenecarboxylic acid methyl ester	–	0.87	–
24.60	Methyl octanoate	1.81	–	1.19
25.75	2,5-Dimethyl-2,4-hexadiene	2.09	0.95	–
28.85	1,1′,1″-(1-ethanyl-2-ylidene)-tris-Benzene	2.69	1.15	–
31.65	1,2-Dimethoxy-4-(3-methoxy-1-propenyl)benzene	–	1.30	–
	All unknown compounds	8.63	6.61	7.11

Reaction conditions: sulfuric acid 1.5 g, material 60 g, methanol 420 g, temperature 200 °C, time 10 min.
[a] Area percent is based on the total ion current.

dimer compounds. The fraction 3# compounds were mainly consisted of 2-methyl-phenol, 4-methyl-guaiacol, 4-methoxy-guaiacol, eugenol, 4-propyl-2,6-dimethoxy-phenol, 4-hydroxy-3-methoxy-phenyl-2-ethanol, vanillin, 4-(3′-methoxy-4′-hydroxy)-phenyl-2-carboxylate, methyl-4-hydroxy-3-methoxy-benzoate, phenols with simple molecular structure and chemical bonding. There were about 10% unknown compounds in the spectra, which could potentially be phenolic trimers, tetramers, and other complex aromatic derivatives. Absolute structural identification of these complex compounds were not possible, since these unknown compounds' aut hentic standards were not available in the GC-MS database.

3.1.3. HSQC NMR spectroscopy of phenolic compounds

2D $^{1}H/^{13}C$ NMR spectroscopy provided some important structural information of complex chemical structure, as it allowed the resolution of otherwise overlapping resonances that observed in the 1D $^{1}H/^{13}C$ NMR spectroscopy. To determine the specific structures in biomass-derived phenolic compounds, as well as the linkages between phenolic compounds and associated side chain groups, all of the three phenolic compounds fractions were analyzed by 2D HSQC NMR spectroscopy in present study. The three phenolic compounds fractions contained phenolic monomers and dimers with various functionalities, such as methyl, methoxy, ether, ester, aldehyde, and complex alkyls. The possible structures and units of three fractions are presented in Fig. S1, included A, B, C, G, H, I, PB, S, and S′ units. In specific, the A, B, C, G, H, I, PB, S, and S′ were on behalf of β-O-4′ ether linkage, resinol unit, phenylcoumaran unit, guaiacyl unit, *p*-hydroxyphenyl unit, *p*-hydroxycinnamyl alcohol unit, *p*-hydroxybenzoate unit, etherified syringyl unit, and oxidized syringyl units, respectively.

The main cross peaks of phenolic compounds fractions in HSQC NMR spectra were presented in Table S4. The whole spectra of phenolic compounds can be divided into three regions: aromatic regions (**A** regions, δ_C/δ_H 95–140/5.00–8.00 ppm), C–O aliphatic side chain regions (**B** regions, δ_C/δ_H 55–90/3.25–6.50 ppm), and C=C aliphatic side chain regions (**C** regions, δ_C/δ_H 15–50/1.00–3.25 ppm) (Fig. S2). The main 2D HSQC correlation signals of three phenolic compounds fractions were shown in Fig. 2, corresponding to the spectra of fraction 1#, 2#, and 3#.

In the **A** region (aromatic region, δ_C/δ_H 95–140/5.00–8.00 ppm), the prominent cross-signals at δ_C/δ_H 130.3–131.1 and 7.55–7.81 correspond to $C_{2,6}/H_{2,6}$ correlations of PB units (Fig. 2 1#-A, 2#-A, 3#-A). Different correlations observed at δ_C/δ_H 114.3/6.41 and 116.3/6.62–6.81 ppm are attributed to C_5/H_5 and C_6/H_6 from G units. The correlation signals at δ_C/δ_H 108.5/7.07 ppm are correlated with $C_{2,6}/H_{2,6}$ correlations of S′ units. The correlation signals at δ_C/δ_H 105.5–106.5 and 6.40–6.50 ppm are attributed to $C_{2,6}/H_{2,6}$ correlations of S units. Besides, minor C_α/H_α aromatic correlation from I units can be observed at δ_C/δ_H 128.4/6.54 in HSQC spectra (Fig. 2 1#-A). In accordance with the HSQC spectra aromatic regions of fractions 2# and 3# (Fig. 2 2#-A, 3#-A), no C_α/H_α correlations of I units were detected. The spectra of fraction 2# have higher ratio of G units than fractions 1# and 3#. Correlation signals for the fraction 2# were much broader than these in the fractions 1# and 3#, which were consistent with its slower molecular motion and higher molecular weights. The signals for S′ units are only presented at the fraction 1#. And there are no correlation signals of S′ and S units in fraction 2#. Only G and PB units were observed in the **A** region of all the three phenolic compounds fractions. Due to the interaction of other functional groups that produced during liquefaction process, the **A** region of three phenolic compounds fractions are obviously different on the altered side chain of the G, PB, S, and S′ aromatic rings.

The **B** regions (C–O aliphatic side-chain region, δ_C/δ_H 55–90/3.25–6.50 ppm) in 2D HSQC spectra also provide useful information about the interunit linkages of these phenolic compounds. Correlation signals for methoxyls (δ_C/δ_H 53.5–57.5/3.55–4.00) and β-O-4′ aryl ether linkages of phenolic compounds are the most prominent in the **B** region. Lignin is composed of randomly branched units of syringols, guaiacols, and phenylpropenyl. The phenylpropenyl, syringols, and guaiacols building blocks, as well as the monomer-derived units, are connected through several types of C–O–C and C–C linkages, including β-O-4, 4-O-5, β-5, β-β, and 5-5, forming biphenyl, resinol, alkyl-aryl ether, phenyl coumarane, and biphenyl ether substructures. The β-O-4 and β-O-4′ linkages are mainly involved in the predominant β-aryl ether units in the natural lignin [40]. And the β-aryl ether units have feature signals at δ_C/δ_H 86.8/5.46 for C_α/H_α, δ_C/δ_H 53.3/3.46 and 53.5/3.06 for C_β/H_β, and δ_C/δ_H 59.5–59.7/3.40–3.63, 61.4/4.10, and 62.5/3.73 for C_γ/H_γ. These correlation signals, along with the corresponding to feature signals from A, B, and C units, could be clearly observed in the spectra from fractions 1# and 2# (Fig. 2 1#-B and 2#-B). However, these correlation signals could not be observed at the spectra of fraction 3# (Fig. 2 3#-B). Herein, we speculate that the phenolic compounds in fraction 3# are mostly single-aromatic-ring phenolic compounds with the smallest molecule-weight products. This result is in accordance with previous thermochemical biomass studies that ether-bonds in cyclic resinols, and phenyl coumarans, β-O-4-linkages in β-ethers can break into small molecule chemicals after thermochemical conversion process [41]. In the **B** region, fraction 3# presents obvious signals at δ_C/δ_H 61.4/4.10 for I units, whereas the spectra of fractions 1# and 2# do not have these cross-signals. The spectra of fraction 1# show prominent signals at δ_C/δ_H 53.5/3.06 for B units, whereas these of fractions 2# and 3# do not have these correlation signals. These results suggest that the C–O linkages in three phenolic compounds fractions are different, and the smallest molecule structures (A, C, and I aromatic units) are separated in fraction 3#. The **C** region (C–C aliphatic side chain region, δ_C/δ_H 15–50/1.00–3.25 ppm) of 2D HSQC spectra from three phenolic compounds fractions are shown in Fig. S3. The signal intensity in **C** region was lower than the **B** region. Fractions 2# and 3# showed similar correlation signals spectra in the **C** region. The cross-signals at δ_C/δ_H 25.3/1.82–1.68 due to $-COCH_3$, along with these corresponding to the feature signals from phenolic units, were clearly observed in fractions 2# and 3#. There is only the solvent DMSO-d_6 signal in fraction 1#.

Based on these HSQC spectra results, we supposed that the primarily aromatic units in three phenolic compounds fractions were G, PB, and S, with minor amounts of H. In this study, HSQC correlation characteristic signals in the aromatic region corresponding to G and PB units were obviously evident in all of the three phenolic compounds fractions, S units were clear in fractions 1# and 2#. In particular, there were only single-aromatic-ring units in the phenolic compounds fraction 3#, which were coincided with the GPC results (Fig. S4 and Table S5). In the aromatic region, the absence of A, B, and C units in the three phenolic compound fractions indicated that depolymerization of lignin occurred during the biomass liquefaction process.

3.1.4. Solubility of phenolic compounds in conventional solvents

Lignocellulosic biomass usually has poor solubility in conventional solvents due to its multi-hydrophilic groups and high degree of polymerization. This difficulty emerged because of the complicated three dimensional lignin network in biomass is interlinked with other components and binds in the entire wood matrix. As a result, the insolubility of lignocellulosic biomass in conventional organic solvents has severely inhibited efforts to produce value-added chemical products, as their poor molecular interaction with other solvent reagents. In this study, the three main

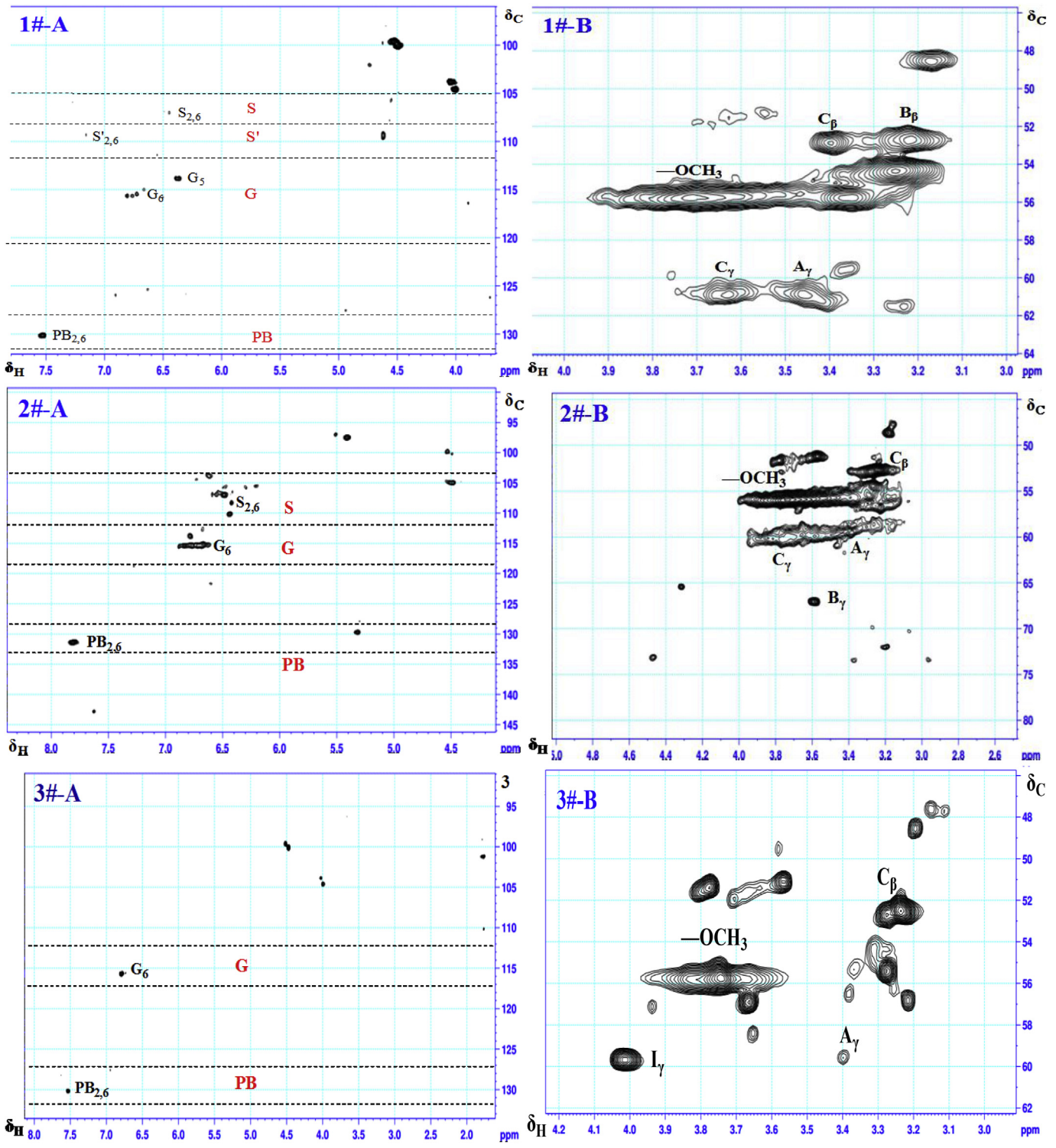

Fig. 2. The HSQC NMR spectra for phenolic compounds in fractions 1#, 2#, and 3#. (A: β-O-4′ ether linkage; B: resinol units; C: phenylcoumaran units; G: guaiacyl units; I: *p*-hydroxycinnamyl alcohol units; PB: *p*-hydroxybenzoate units; S: etherified syringyl units; S′: oxidized syringyl units.)

components (lignin, hemicelluloses, and cellulose) in lignocellulosic biomass were decomposed into lower fragments such as phenolic compounds and sugar derivatives. The solubility of these products was significantly enhanced due to their low-weight molecular and low-size molecular. The solubility of phenolic compounds derived from liquefied products was tested using several conventional organic solvents. For comparative purpose, the solubility of pure lignin in organic solvents was also tested.

As shown in Fig. 3, the phenolic compounds from liquefaction can be completely dissolved in organic solvents such as tetrahydrofuran and acetone, while pure lignin is completely insoluble in these solvents. Model phenolic compounds, such as phenol and guaiacol, can also be easily dissolved in tetrahydrofuran and acetone. These results suggest that phenolic compounds from

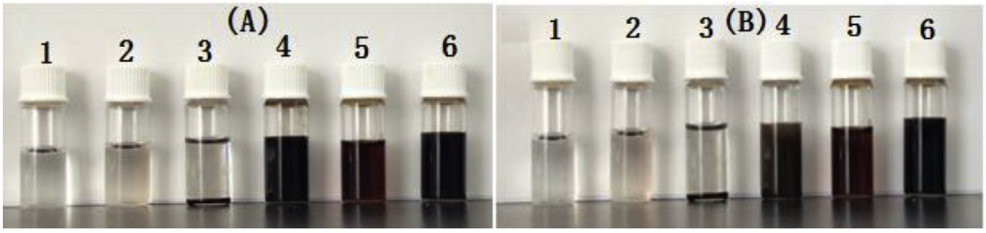

Fig. 3. The solubility of various phenolic compounds in organic solvents at ambient temperature. (Phenol (1), guaiacol (2), pure lignin (3), fraction 1# (4), fraction 2# (5), and fraction 3# (6) in tetrahydrofuran(A) and acetone(B)).

liquefied products should have better chemical reactivity because a homogeneous phase reaction system can be formed in many reactions by conventional organic solvents. The phenolic compounds from liquefaction have low molecular weight, which corresponding to an increasing probability of molecular collision with reactants. And the phenolic compounds also have lower molecular size, which providing a potential reaction activity with other reactants, because they had only minor steric hindrance compared with pure lignin.

3.1.5. FT-IR analysis of phenolic compounds and liquefied products

Both phenolic compounds and liquefied products contained hydroxyl, carbonyl groups, carbon–carbon double bonds, and aromatic rings. The liquefaction and alcoholysis of bamboo was not only cellulose and hemicellulose degrading into glycosides, but also the decomposition of high molecular polymerization lignin into phenolic compounds. The reactive intermediates compose of carbon–carbon double bonds, hydroxyl and/or carbonyl groups. The major linkages between the structural units of natural lignin in biomass are β-O-4 (β-aryl ether), β-β (resinol), and β-5 (phenylcoumaran).

To evaluate the three phenolic compounds fractions and original liquefied products, the FT-IR spectroscopy was used to analyse the liquefied products and phenolic compounds throughout the reaction process (Fig. 4). The assignments of the peaks are summarized in Table S6. By comparing the FT-IR spectra of liquefied products with phenolic compounds, the broad peak at around 3350 cm^{-1} represents the –OH groups derived from lignin or cellulose. The peaks at approximately 2930 and 2850 cm^{-1} represent C–H in a symmetric stretching of aliphatic methyl. And a band appearing at around 1600 cm^{-1} is characteristic of C=C skeleton vibration in aromatic skeletal of lignin or phenols. This peak is a weak absorption band observed in liquefied products, indicated the three phenolic compounds fractions can be successfully concentrated after the stepwise precipitation and extraction. In three phenolic compounds fractions, the peak at approximately 1260 cm^{-1} represents C–O stretching vibration in phenolic hydroxyl group.

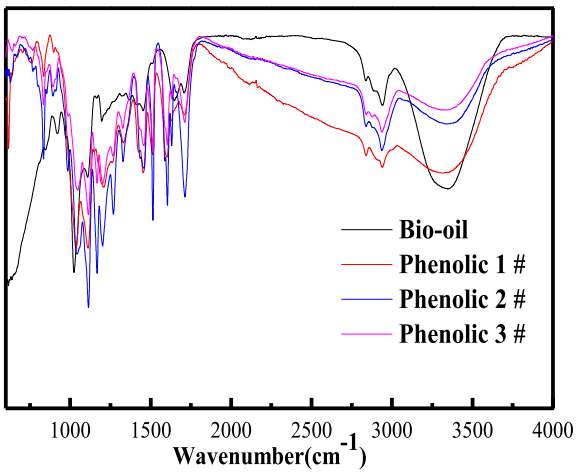

Fig. 4. FT-IR analysis of three phenolic compounds fraction (1#, 2#, 3#) and bio-oil. (Bio-oil is come from liquefied products with all methanol has been removed by vacuum distillation at 50 °C.)

3.2. In situ hydrodeoxygenation of phenolic compounds over bifunctional catalysts

3.2.1. Different hydrodeoxygenation process of model phenolics

Bifunctional catalysts, containing both acid and metal components, were applied to solve the deactivation problem caused by the traditional hydrodeoxygenation catalysts. Zhao [34] reported that a bifunctional catalyst combined Pd/C, Rh/C, Pt/C, or Ru/C with H_3PO_4 could selectively catalyze the hydrodeoxygenation of phenols into alkanes. During the hydrodeoxygenation, both the metal-catalyzed hydrogenation and acid-catalyzed dehydration/hydrolysis were happened. The systematic kinetic study revealed that the bifunctional catalytic functions are necessary [43], and the acid-catalyzed step can determine the overall hydrodeoxygenation reaction. Therefore, high concentrations of acid sites were required in efficient hydrodeoxygenation process. Solid Brönsted acids were found effective for hydrodeoxygenation of phenols with the bifunctional catalysts combination [43,44]. Compared to other studied solid acids (such as Amberlyst 15, Nafion/SiO_2, and sulfated zirconia), HZSM-5 showed a higher reaction rate, due to its higher acid concentrations in the zeolite pores [43]. Ni-based hydrogenation catalysts such as Raney Ni combined with Nafion (or SiO_2) [44] or Ni/HZSM-5 [33], instead of precious metal catalysts, were also effective in the bifunctional hydrodeoxygenation catalysts system. The hydrogenation of phenolic compounds was the determining rate step in the Ni/HZSM-5 system, hence, high Ni dispersions were required in efficient catalysis.

Considering the mentioned upgrading catalysts of phenolic compounds, Raney Ni and HZSM-5 were chosen as the bifunctional catalysts for hydrodeoxygenation of lignin-derived phenolic compounds. And the characterization of bifunctional catalysts (Raney Ni and HZSM-5) was shown in Table S7 and Fig. S5. In our study, Raney Ni can catalyze the aqueous-phase reforming of methanol to produce the hydrogen. The aqueous phase reforming of methanol to produce hydrogen could partly avoid the abrasion of reactor and risk of operation. And in the *in situ* hydrodeoxygenation, the combination of Raney Ni and HZSM-5 can catalyse the hydrodeoxygenation of phenolic monomers and phenolic dimers. The latter one required a cascade metal-catalyzed and acid-catalyzed cleavage of C–O bonds (α-O-4, β-O-4, 4-O-5, etc.), and integrated hydrogenation and dehydration reactions (Table 3). The product cyclohexanes and their derivatives can be easily separated from solvent since they are immiscible. In general, the *in-situ* hydrodeoxygenation over the bifunctional catalysts Raney Ni and HZSM-

5, can effectively convert the phenolic compounds into cyclohexanes and hydrocarbons with high conversion of phenolic compounds and selectively of cyclohexanes. This could actually comprise the process of hydrodeoxygenation and supply an efficient pathway for refining and upgrading the biomass-derived phenolic compounds and bio-oils.

3.2.2. *In situ hydrodeoxygenation of biomass-derived phenolic compound*

The liquefied products from hemicellulose and cellulose high contents of relatively small oxygenates, such as furfurals, glycosides and their derivatives (Table S8 and Fig. S6), can be used as high added-value chemicals. However, lignin decomposes the polymer leading to higher concentration of phenolic compounds. The upgrading of phenolic compounds is a critical step before the valorization of liquefied lignin. A sustainable hydrodeoxygenation which involved *in situ* catalytic hydrodeoxygenation of phenolic compounds (separated from bio-oil) for producing cyclohexanes and hydrocarbons bio-fuel has been investigated in detail. The process of aqueous-phase reforming of methanol coupled with the *in situ* hydrodeoxygenation of phenolic compounds has been discussed.

The one-pot *in situ* hydrodeoxygenation procedure is carried out in the presence of Raney Ni and HZSM-5 using methanol as a hydrogen donor. The water and methanol were used to generate H_2 through the aqueous phase reforming in the *in situ* hydrodeoxygenation. The H_2 produced by water and methanol components is sufficient for selective hydrodeoxygenation of the phenolic compounds to hydrocarbon fuels. The gas products of hydrodeoxygenation showed that about 35% of H_2 and more 30% of CH_4, and a minute amount of C_2H_6 and C_3H_8 hydrocarbons were obtained (Table S9). No solid products were found after the *in situ* hydrodeoxygenation.

The major components and relative contents of upgraded phenolic fractions after *in situ* hydrodeoxygenation were shown by peak area % are given in Table 4 and Fig. 5, respectively. Compared with Table 2, it can be seen that after *in situ* hydrodeoxygenation upgrading at this mild condition, a series of cyclohexane hydrocarbons and derivatives were obtained, and few phenolic compounds were detected. However, it should be mentioned that quantities of cyclohexanol derivatives were also found such as 2-methoxy-cyclohexanol, 2-methoxy-4-methyl-cyclohexanol, and 2-methyl-cyclohexanone. It should also be noted that the C5–C9 hydrocarbon products mainly occupied the distribution of the corresponding upgrading components.

In summary, the original bifunctional catalysts combined Raney Ni with HZSM-5 to achieve aqueous-phase reforming of methanol coupled with the *in situ* hydrogenation of phenolic compounds. The combination of Raney Ni and HZSM-5 in the *in situ* hydrodeoxygenation was effective at removing oxygen-containing groups (ketones, hydroxyl, methoxy, aryl-O-aryl, and alkyl-O-aryl) in three phenolic compounds fractions with water and methanol at 220 °C. That demonstrated the bifunctional catalytic effect of the acid and metal together is required to break down these stable bonds.

The mechanism of *in situ* hydrodeoxygenation of different phenolic compounds is proposed in Fig. 6. The Raney Ni mainly catalysed the reaction of aqueous phase reforming of methanol to produce H_2 and the reaction of phenolic compounds hydrogenated into cyclohexanol derivatives. The Brønsted acid HZSM-5 was applied to the dehydration of cyclohexanol. HZSM-5 is hydrothermally stable and does not deactivate over a significant number of reaction cycles. Since water is used as the solvent for this process, hydrocarbon products are easily collected by phase separation. Overall, the bifunctional catalysts can integrate the hydrogenation and dehydration of biomass-derived phenolic compounds through the *in situ* hydrodeoxygenation. This approach supplies an efficient route for upgrading lignin-derived phenolic oil into fuel additives and liquid hydrocarbons.

3.3. *Chemical analysis of residue*

SEM pictures of the bamboo and liquefied residue are shown in Fig. 7. With reaction processing, the surface of the residual fibres was irregular and contained many small fragments of cell wall components in Fig. 7 (a partially enlarged image). Most small fragments attached on the surface of the fibres have been removed, but the residue was largely maintained on its original fiber bundles. This phenomenon indicated that the liquefied residue was the cellulose framework, and the hemicellulose and lignin had been mostly decomposed. It was very difficult for the organic solvent to infiltrate this high density crystallized cellulose skeleton under the reaction conditions. Although more severe reaction conditions can increase the conversion of biomass, the better solution may be to use a water vapour explosion pre-treatment to obtain higher reaction surface area.

To examine the effect of crystallinity on cellulose decomposition, XRD analysis was performed on residue and bamboo. Fig. S7

Table 3
Different hydrodeoxygenation process of model compounds over bifunctional catalysts.

Catalyst	Reaction conditions			Models	Major products	Sele. (%)	Conv. (%)	Ref.
	T (°C)	P (MPa)	Solvent					
Pd/C + H_3PO_4	250	5 (H_2)	H_2O	Phenol	Cyclohexane	98	100	[42]
				4-Methylguaiacol	Methyl cyclohexane	78	100	[42]
Pd/C + HZSM-5	200	5 (H_2)	H_2O	Phenol	Cyclohexane	100	100	[43]
				4-Methylguaiacol	Methyl cyclohexane	100	88	[43]
Raney Ni + Nafion/SiO_2	300	4 (H_2)	H_2O	Phenol	Cyclohexane	100	93	[44]
				4-Methylguaiacol	Methyl cyclohexane	100	74	[44]
				4-Propylphenol	4-Propy cyclohexane	100	92	[44]
Ni/HZSM-5	250	5 (H_2)	H_2O	Guaiacol	Cyclohexane	100	74	[33]
				4-Methylguaiacol	Methyl cyclohexane	100	73	[33]
Raney Ni + HBEA-35	150	0	2-PrOH–n-$C_{16}H_{34}$	Phenol	Benzene	82	100	[45]
Raney Ni + HZSM-5[a]	220	0.1(N_2)	MeOH–H_2O	Phenol	Cyclohexane	100	100	
				Guaiacol	Cyclohexane	100	94	
				4-Methylguaiacol	Methyl cyclohexane	100	90	
				4-(Benzyloxy)-phenol(α-O-4)	Cyclohexane and its derivatives	87	98	
				1-Phenethoxy-benzene (β-O-4)	Cyclohexane and its derivatives	85	96	
				1-Phenoxy-benzene(4-O-5)	Cyclohexane and its derivatives	78	99	

[a] Reaction conditions: model phenolics 2.0 g, methanol 10 g, water 20 g, temperature 220 °C, time 9 h, p_0 0.1 MPa.

Table 4
Components of three phenolic compounds fractions after *in situ* hydrodeoxygenation.

R.T. (min)	Identification by GC-MS	Peak area (%)[a]		
		1#	2#	3#
	Cyclohexanes, cyclohexanols	**53.90**	**60.15**	**65.67**
3.78	Cyclohexane	13.43	11.17	13.33
4.49	Methyl-cyclohexane	2.27	5.64	7.92
6.98	2-Methoxy-cyclohexanol	6.14	4.82	6.21
7.65	Cyclohexanol	2.95	7.78	6.23
8.01	4-Propylcyclohexane	9.95	4.31	5.11
8.73	2-Methyl-cyclohexanone	7.42	9.68	5.23
9.64	Bicyclohexane	1.32	0.92	4.35
10.29	2-Methyl-cyclohexanol	3.54	4.43	3.09
11.32	2-Methoxy-4-methyl-cyclohexanol	2.31	6.21	7.61
12.81	3-Methylcyclopentane-1,2-diol	1.05	–	0.21
14.82	Hydroxy-cyclohexanone	–	0.37	5.21
15.17	4-Propylcyclohexanol	3.52	4.82	1.17
	Phenolic compounds	**36.15**	**32.89**	**20.11**
9.21	Phenol	0.89	0.78	0.21
10.67	2-Methyl-phenol	0.21	–	0.17
12.08	4-Propyl-phenol	0.45	0.42	1.07
13.47	Guaiacol	2.07	–	3.02
16.69	3-Methyl-guaiacol	–	1.01	2.03
18.09	4-Methoxy-guaiacol	2.59	2.44	0.31
19.46	Catechol	1.32	5.31	–
20.27	4-Propyl-2,6-dimethoxyphenol	1.57	4.09	3.19
20.95	4-Hydroxy-3-methoxyphenyl-2-ethanol	2.26	4.14	3.61
23.66	2-methoxy-4-acetone-phenol	8.18	3.98	–
25.39	Vanillin	2.60	–	2.04
26.47	4-(3′-methoxy-4′-hydroxy)-phenyl-2-carboxylate	7.28	4.15	4.08
29.80	4-(3′-methoxy-4′-hydroxy)-phenyl-2-butenoate	4.22	2.19	–
30.62	Apocynol	0.78	0.59	–
31.52	4-Methoxy-2-hydroxybenzoate	1.28	3.01	0.38
33.51	Phenolic dimers	0.45	0.78	–
	Others	9.95	6.96	14.22

Reaction conditions: phenolic compounds 2.0 g, methanol 10 g, water 20 g, temperature 220 °C, time 9 h, p_0 0.1 MPa.
[a] Area percent is based on the total ion current.

represents a diffraction pattern with 2θ that varies from 10° to 60°. Three broad peaks were observed at the 2θ values at around 16°, 22°, and 35° for residue and bamboo, which represented 101, 002, and 040 lattice spacing in the cellulose of wood [46]. Compared with bamboo, the peaks became narrow and low in residue. According to Eq. (2), we calculated the relative crystallinity of the raw material and liquefied residue. The results were 43.75% and 48.49%. These results suggest that the liquefied process increased the relative crystallinity of the residue because the cellulose in non-crystalline region (amorphous region) decreased more than the cellulose in the crystalline region. In general, increased relative crystallinity showed some dependency on cellulose decomposition, which was in agreement with the SEM result.

TG distribution against temperature for residue and bamboo is shown in Fig. 8(a). As the temperature increased, the pyrolysis process experienced four steps. At the first stage, the drying stage of the samples occurred from 30 to 130 °C, and the weight of water gradually decreased as did the samples mass. At the second stage, the warm-up phase of pyrolysis is in a temperature range of 140–260 °C. The raw material depolymerization and "glass" state transition reactions have occurred. The main pyrolysis process in the third stage is from 260 to 400 °C. Both bamboo and residue were converted into low molecular gas and macromolecular condensable volatiles which caused significant weight loss [47]. At the last stage, the carbonized fiber stage of samples ranged from 400 to 800 °C. There was a clear exothermic peak corresponding to the slow decomposition of the remaining material pyrolysis, which generated carbon residue and ash. DTG distribution against temperature for residue and bamboo are shown in Fig. 8 (b). The change in the liquefied process of bamboo and residue was mostly similar. In the first and second stages, the weight loss of bamboo was more obvious than residue due to structural differences. Also, the moisture content of bamboo was higher than the residue. In the third stage, while the weight loss of residue was more obvious than bamboo, the residue at 337.5 °C weight lost rate reached a maximum of −17.93%/min. Bamboo at 341 °C weight loss rate reached a maximum of −10.01%/min. The fourth stage, the pyrolysis residual of bamboo and residue were 23.33% and 12.49%, respectively.

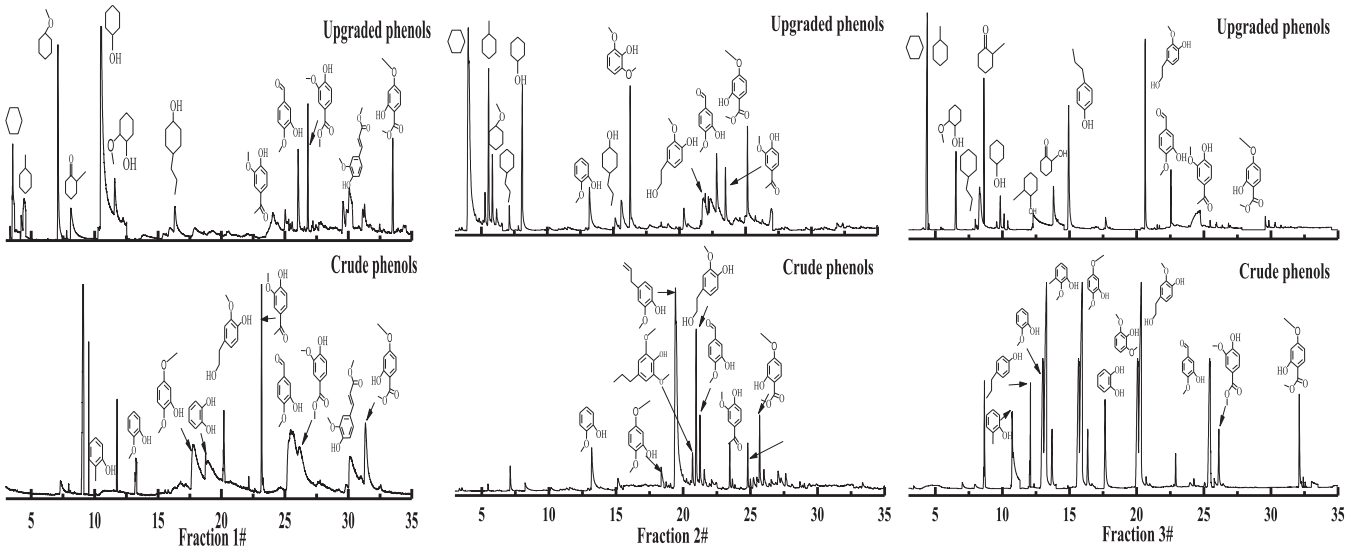

Fig. 5. GC-MS of three phenolic compounds fractions before and after *in situ* hydrodeoxygenation.

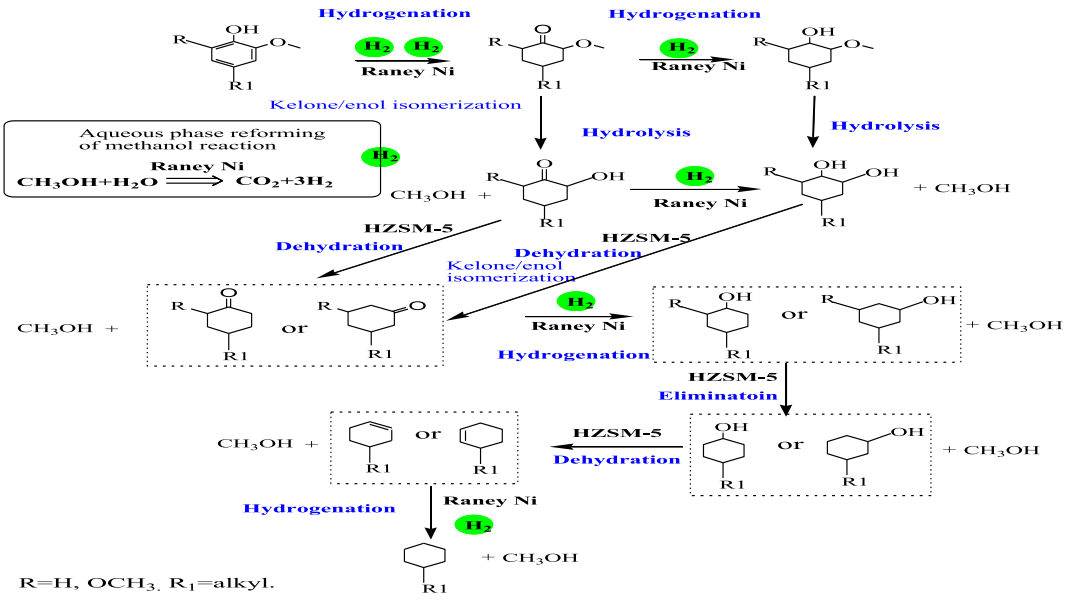

Fig. 6. Proposed mechanism of *in situ* hydrodeoxygenation of phenolic compounds.

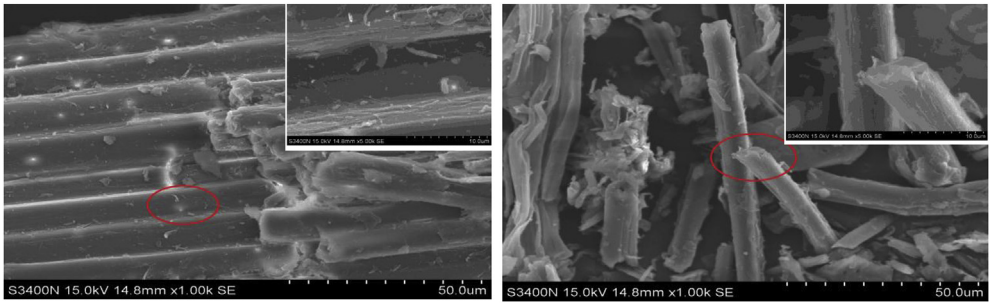

Fig. 7. SEM pictures for bamboo material (left) and liquefied residue (right).

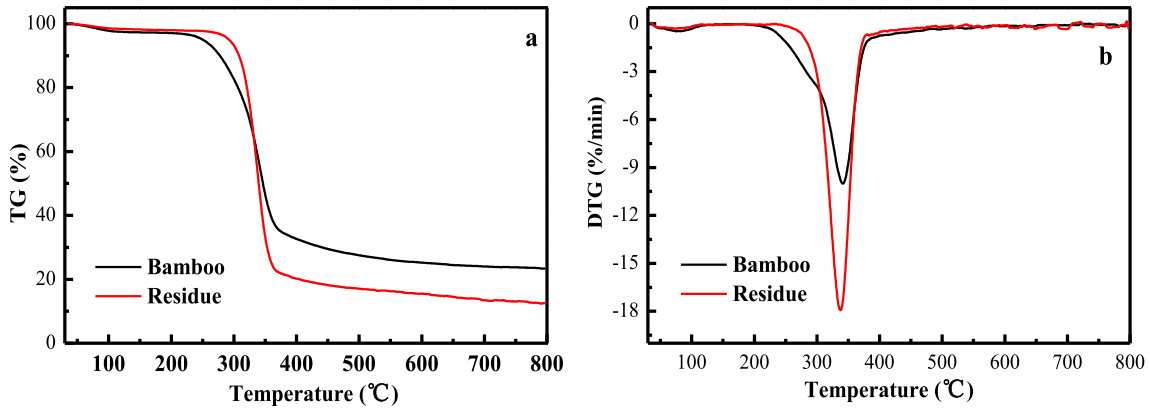

Fig. 8. TG (a) and DTG (b) analysis of bamboo material and liquefied residue.

4. Conclusions

This study presents the promising process for extracting three phenolic compound fractions via stepwise precipitation and extraction of liquefied biomass, and upgrading these three phenolic compounds fractions into organic cyclohexanes. The directional liquefaction of lignocellulosic biomass was conducted in methanol with acid catalyst, and the conversion of materials were about 80%. After liquefaction, the liquefied oil were separated by water and organic solvent with a stepwise precipitation and extraction process. The phenolic compounds with high purity can be achieved by stepwise process of liquefied products. Three phenolic compounds fractions were mainly comprised of 4-methyl-guaiacol, 4-methoxy-guaiacol, eugenol, 4-hydroxy-3-methoxyphenyl-2-ethanol, 4-methoxy-2-hydroxybenzoate, and (E)-methyl-3-(4-hydroxy-3-methoxyphenyl) acrylate. Three phenolic compound fractions had

a good solubility in conventional organic solvents, which indicated these phenolic compounds had a potential reactivity with other reagents. We investigated the *in situ* catalytic hydrodeoxygenation of these phenolic compounds to cyclohexanes and hydrocarbons compounds with methanol and water over bifunctional catalysts. The bifunctional catalysts combined Raney Ni with HZSM-5 can achieve aqueous-phase reforming of methanol coupled with the *in situ* hydrogenation of phenolic compounds. The bifunctional catalysts showed high selectivity in removing oxygen-containing groups in biomass-derived phenolic compounds through *in situ* hydrodeoxygenation. Therefore, the cascade bifunctional catalysts can integrate aqueous-phase reforming of methanol, hydrogenation, and dehydration of biomass-derived phenolic compounds. The *in situ* hydrodeoxygenation of phenolic compounds can prepare liquid cyclohexanes and cyclohexane hydrocarbons, provide a more efficient and less energy-demanding upgrading process. Overall, this stepwise precipitation and *in situ* hydrodeoxygenation system can convert lignocellulosic biomass into renewable hydrocarbons.

Acknowledgements

The authors thank the Research Institute of New Technology at Chinese Academy of Forestry-Special Fund for Fundamental Research (CAFYBB2014ZD003) and the Natural Science Foundation of Jiangsu Province (BK20151068). The authors gratefully acknowledge the financial support provided by the National Natural Science Foundation of China (31530010 and 31422013) for this investigation.

Appendix A. Supplementary data

Supplementary data related to this article can be found at http://dx.doi.org/10.1016/j.energy.2017.06.032.

References

[1] Limayem A, Ricke SC. Lignocellulosic biomass for bioethanol production: current perspectives, potential issues and future prospects. Prog Energy Combust 2012;38(4):449–67.
[2] Wang K, Kim KH, Brown RC. Catalytic pyrolysis of individual components of lignocellulosic biomass. Green Chem 2014;16(2):727–35.
[3] Zhou CH, Xia X, Lin CX, Tong DS, Beltramini J. Catalytic conversion of lignocellulosic biomass to fine chemicals and fuel. Chem Soc Rev 2011;40(11):5588–617.
[4] Shuai L, Amiri MT, Questell-Santiago YM, Héroguel F, Li Y, Kim H, et al. Formaldehyde stabilization facilitates lignin monomer production during biomass depolymerization. Science 2016;354(6310):329–33.
[5] Burguete P, Corma A, Hitzl M, Modrego R, Ponce E, Renz M. Fuel and chemicals from wet lignocellulosic biomass waste streams by hydrothermal carbonization. Green Chem 2016;18(4):1051–60.
[6] Bhagavatula A, Shah N, Honaker R. Estimating the pyrolysis kinetic parameters of coal, biomass, and their blends: a comparative study. Energy Fuels 2016;30(12):10045–54.
[7] Alonso DM, Bond JQ, Dumesic JA. Catalytic conversion of biomass to biofuels. Green Chem 2010;12(9):1493–513.
[8] Liu C, Wang H, Karim AM, Sun J, Wang Y. Catalytic fast pyrolysis of lignocellulosic biomass. Chem Soc Rev 2014;43(22):7594–623.
[9] Zhang B, Zhong Z, Chen P, Ruan R. Microwave-assisted catalytic fast pyrolysis of biomass for bio-oil production using chemical vapor deposition modified HZSM-5 catalyst. Bioresour Technol 2015;197:79–84.
[10] Zhu Y, Biddy MJ, Jones SB, Elliott DC, Schmidt AJ. Techno-economic analysis of liquid fuel production from woody biomass via hydrothermal liquefaction (HTL) and upgrading. Appl Energy 2014;129:384–94.
[11] Climent MJ, Corma A, Iborra S. Conversion of biomass platform molecules into fuel additives and liquid hydrocarbon fuels. Green Chem 2014;16(2):516–47.
[12] Yan X, Wang B, Zhang J. Liquefaction of cotton seed in sub-critical water/ethanol with modified medical stone for bio-oil. Bioresour Technol 2015;197:120–7.
[13] Trautmann M, Löwe A, Traa Y. An alternative method for the production of second-generation biofuels. Green Chem 2014;16(8):3710–4.
[14] Sanna A, Vispute TP, Huber GW. Hydrodeoxygenation of the aqueous fraction of bio-oil with Ru/C and Pt/C catalysts. Appl Catal B Environ 2015;165:446–56.
[15] Grilc M, Likozar B, Levec J. Hydrodeoxygenation and hydrocracking of solvolysed lignocellulosic biomass by oxide, reduced and sulphide form of NiMo, Ni, Mo and Pd catalysts. Appl Catal B Environ 2014;150:275–87.
[16] Pang K, Hou Y, Wu W, Guo W, Peng W, Marsh KN. Efficient separation of phenols from oils via forming deep eutectic solvents. Green Chem 2012;14(9):2398–401.
[17] Vasco CA, Ma R, Quintero M, Guo M, Geleynse S, Ramasamy KK, et al. Unique low-molecular-weight lignin with high purity extracted from wood by deep eutectic solvents (DES): a source of lignin for valorization. Green Chem 2016;18(19):5133–41.
[18] Yao G, Wu G, Dai W, Guan N, Li L. Hydrodeoxygenation of lignin-derived phenolic compounds over bi-functional Ru/H-beta under mild conditions. Fuel 2015;150:175–83.
[19] Pittman Jr CU, Mohan D, Eseyin A, Li Q, Ingram L, Hassan EBM, et al. Characterization of bio-oils produced from fast pyrolysis of corn stalks in an auger reactor. Energy Fuel 2012;26(6):3816–25.
[20] Vitasari CR, Meindersma GW, De Haan AB. Water extraction of pyrolysis oil: the first step for the recovery of renewable chemicals. Bioresour Technol 2011;102(14):7204–10.
[21] Guo X, Wang S, Guo Z, Liu Q, Luo Z, Cen K. Pyrolysis characteristics of bio-oil fractions separated by molecular distillation. Appl Energy 2010;87(9):2892–8.
[22] Wang Y, Wang S, Leng F, Chen J, Zhu L, Luo Z. Separation and characterization of pyrolytic lignins from the heavy fraction of bio-oil by molecular distillation. Sep Purif Technol 2015;152:123–32.
[23] Wei Y, Lei H, Wang L, Zhu L, Zhang X, Liu Y, et al. Liquid-liquid extraction of biomass pyrolysis bio-oil. Energy Fuel 2014;28(2):1207–12.
[24] Patel RN, Bandyopadhyay S, Ganesh A. Extraction of cardanol and phenol from bio-oils obtained through vacuum pyrolysis of biomass using supercritical fluid extraction. Energy 2011;36(3):1535–42.
[25] Dobele G, Dizhbite T, Ponomarenko J, Urbanovich I, Kreicberga J, Kampars V. Isolation and characterization of the phenolic fractions of wood pyrolytic oil. Holzforschung 2011;65(4):503–10.
[26] Elliott DC, Wang H, Rover M, Whitmer L, Smith R, Brown R. Hydrocarbon liquid production via catalytic hydroprocessing of phenolic oils fractionated from pyrolysis of red oak and corn stover. ACS Sustain Chem Eng 2015;3(5):892–902.
[27] De S, Saha B, Luque R. Hydrodeoxygenation processes: advances on catalytic transformations of biomass-derived platform chemicals into hydrocarbon fuels. Bioresour Technol 2015;178:108–18.
[28] Besse X, Schuurman Y, Guilhaume N. Hydrothermal conversion of lignin model compound eugenol. Catal Today 2015;258:270–5.
[29] Cordero-Lanzac T, Palos R, Arandes JM, Castaño P, Rodríguez-Mirasol J, Cordero T, et al. Stability of an acid activated carbon based bifunctional catalyst for the raw bio-oil hydrodeoxygenation. Appl Catal B Environ 2017;203:389–99.
[30] Zhu X, Lobban LL, Mallinson RG, Resasco DE. Bifunctional transalkylation and hydrodeoxygenation of anisole over a Pt/HBeta catalyst. J Catal 2011;281(1):21–9.
[31] Yao G, Wu G, Dai W, Guan N, Li L. Hydrodeoxygenation of lignin-derived phenolic compounds over bi-functional Ru/H-Beta under mild conditions. Fuel 2015;150:175–83.
[32] Zhang W, Chen J, Liu R, Wang S, Chen L, Li K. Hydrodeoxygenation of lignin-derived phenolic monomers and dimers to alkane fuels over bifunctional zeolite-supported metal catalysts. ACS Sustain Chem Eng 2014;2(4):683–91.
[33] Zhao C, Lercher JA. Upgrading pyrolysis oil over Ni/HZSM-5 by cascade reactions. Angew Chem 2012;124(24):6037–42.
[34] Zhao C, Kou Y, Lemonidou AA, Li X, Lercher JA. Highly selective catalytic conversion of phenolic bio-oil to alkanes. Angew Chem 2009;121(22):4047–50.
[35] He J, Zhao C, Lercher JA. Impact of solvent for individual steps of phenol hydrodeoxygenation with Pd/C and HZSM-5 as catalysts. J Catal 2014;309:362–75.
[36] Vasiliadou ES, Yfanti VL, Lemonidou AA. One-pot tandem processing of glycerol stream to 1, 2-propanediol with methanol reforming as hydrogen donor reaction. Appl Catal B Environ 2015;163:258–66.
[37] Ferrini P, Rinaldi R. Catalytic biorefining of plant biomass to non-pyrolytic lignin bio-oil and carbohydrates through hydrogen transfer reactions. Angew Chem 2014;53(33):8634–9.
[38] Xu J, Xie X, Wang J, Jiang J. Directional liquefaction coupling fractionation of lignocellulosic biomass for platform chemicals. Green Chem 2016;18:3124–38.
[39] Zakzeski J, Bruijnincx PC, Jongerius AL, Weckhuysen BM. The catalytic valorization of lignin for the production of renewable chemicals. Chem Rev 2010;110(6):3552–99.
[40] Chen W, McClelland DJ, Azarpira A, Ralph J, Luo Z, Huber GW. Low temperature hydrogenation of pyrolytic lignin over Ru/TiO_2: 2D HSQC and ^{13}C NMR study of reactants and products. Green Chem 2016;18(1):271–81.
[41] Chu S, Subrahmanyam AV, Huber GW. The pyrolysis chemistry of a β-O-4 type oligomeric lignin model compound. Green Chem 2013;15(1):125–36.
[42] Zhao C, He JY, Lemonidou AA, Li XB, Lercher JA. Aqueous-phase hydrodeoxygenation of bio-derived phenols to cycloalkanes. J Catal 2011;280:8–16.
[43] Zhao C, Lercher JA. Selective hydrodeoxygenation of lignin-derived phenolic monomers and dimers to cycloalkanes on Pd/C and HZSM-5 catalysts.

ChemCatChem 2012;4:64–8.
[44] Zhao C, Kou Y, Lemonidou AA, Li XB, Lercher JA. Hydrodeoxygenation of bio-derived phenols to hydrocarbons using RANEY (R) Ni and Nafion/SiO_2 catalysts. Chem Commun 2010;46:412–4.
[45] Wang X, Rinaldi R. A route for lignin and bio-oil conversion: dehydroxylation of phenols into arenes by catalytic tandem reactions. Angew Chem 2013;52(44):11499–503.
[46] Biswas AK, Umeki K, Yang W, Blasiak W. Change of pyrolysis characteristics and structure of woody biomass due to steam explosion pretreatment. Fuel Process Technol 2011;92(10):1849–54.
[47] Bhagavatula A, Huffman G, Shah N, Romanek C, Honaker R. Source apportionment of carbon during gasification of coal–biomass blends using stable carbon isotope analysis. Fuel Process Technol 2014;128:83–93.